Zero kinetic energy photoelectron spectroscopy of triphenylene

Citation	Harthcock, C., Zhang, J., & Kong, W. (2014). Zero kinetic energy photoelectron spectroscopy of triphenylene. Journal of Chemical Physics, 140(24), 244308. doi:10.1063/1.4884905
DOI	10.1063/1.4884905
Publisher	American Institute of Physics Publishing
Version	Version of Record
Terms of Use	http://cdss.library.oregonstate.edu/sa-termsofuse

Zero kinetic energy photoelectron spectroscopy of triphenylene

Colin Harthcock, Jie Zhang, and Wei Kong[a)]
Department of Chemistry, Oregon State University, Corvallis, Oregon 97331, USA

(Received 30 November 2013; accepted 11 June 2014; published online 26 June 2014)

We report vibrational information of both the first electronically excited state and the ground cationic state of jet-cooled triphenylene via the techniques of resonantly enhanced multiphoton ionization (REMPI) and zero kinetic energy (ZEKE) photoelectron spectroscopy. The first excited electronic state S_1 of the neutral molecule is of A_1' symmetry and is therefore electric dipole forbidden in the D_{3h} group. Consequently, there are no observable Franck-Condon allowed totally symmetric a_1' vibrational bands in the REMPI spectrum. All observed vibrational transitions are due to Herzberg-Teller vibronic coupling to the E′ third electronically excited state S_3. The assignment of all vibrational bands as e′ symmetry is based on comparisons with calculations using the time dependent density functional theory and spectroscopic simulations. When an electron is eliminated, the molecular frame undergoes Jahn-Teller distortion, lowering the point group to C_{2v} and resulting in two nearly degenerate electronic states of A_2 and B_1 symmetry. Here we follow a crude treatment by assuming that all e′ vibrational modes resolve into b_2 and a_1 modes in the C_{2v} molecular frame. Some observed ZEKE transitions are tentatively assigned, and the adiabatic ionization threshold is determined to be 63 365 ± 7 cm^{-1}. The observed ZEKE spectra contain a consistent pattern, with a cluster of transitions centered near the same vibrational level of the cation as that of the intermediate state, roughly consistent with the propensity rule. However, complete assignment of the detailed vibrational structure due to Jahn-Teller coupling requires much more extensive calculations, which will be performed in the future. © *2014 AIP Publishing LLC*. [http://dx.doi.org/10.1063/1.4884905]

INTRODUCTION

Polycyclic aromatic hydrocarbons (PAHs) are a group of molecules consisting of fused benzene rings. They are readily formed during incomplete combustion of fossil fuels and are considered potent pollutants due to their carcinogenic properties.[1–3] PAHs have also been observed in comet tails and are possibly a major component of the interstellar medium (ISM).[4,5] They have been considered responsible for many of the spectroscopic features observed in the ISM and have substantial implications to the energy balance of the universe.[6–13] In astrobiology, it has been hypothesized that PAHs could be related to the origin of life by forming the first primitive organic molecules including amino acids in the pre-DNA world.[14–16]

Many spectroscopic studies of neutral and cationic PAHs have been motivated by astrophysical modeling.[17–22] Both the infrared and visible/ultraviolet regions have been extensively investigated using techniques of photoionization, cavity ring-down, photoabsorption, and photoemission spectroscopy.[21,23–27] Unfortunately, the far-infrared (FIR) region has been largely untouched because of issues related to detector sensitivity and light source intensity. On the other hand, the FIR region is occupied by skeletal vibrations of the molecular frame, and it is considered the "fingerprint region" for spectroscopic identification of astrophysical PAHs.[28,29]

The technique of zero kinetic energy (ZEKE) photoelectron spectroscopy offers an indirect solution to the challenges in the FIR of cations for laboratory astrophysics.[30] In recent years, we have undertaken the mission of mapping out the low frequency vibrational modes of PAHs using ZEKE spectroscopy.[31–37] So far we have reported four peri-condensed species including pyrene, benzo[*a*]pyrene (B*a*P), benzo[*e*]pyrene (B*e*P), and benzo[*g,h,i*]perylene (B*ghi*P) as well as three cata-condensed species including tetracene, pentacene, and chrysene.[31–37] Our results together with previous matrix isolation spectroscopy (MIS)[38–41] and other experimental efforts offer the possibility of a comprehensive analysis of the vibrational modes of a few selected cationic species, thereby benchmarking theoretical calculations and astrophysical modeling.

In this work, we report our new results on triphenylene, a highly symmetric neutral molecule with D_{3h} symmetry. The first electronically excited state S_1 of triphenylene is electric dipole forbidden,[38,39] hence all vibronic transitions originate from Herzberg-Teller (HT) vibronic coupling during resonantly enhanced multiphoton ionization (REMPI). The cationic state, on the other hand, is believed to be of C_{2v} symmetry, undergoing Jahn-Teller (JT) distortion when an electron is eliminated from the molecular frame.[42–44] We offer vibrational analysis of both the REMPI and ZEKE spectra, and discuss the role of symmetry in affecting the vibronic activities of the system.

a)Author to whom correspondence should be addressed. Electronic mail: wei.kong@oregonstate.edu. Tel.: 541-737-6714.

EXPERIMENTAL SETUP AND CALCULATION METHOD

The experimental apparatus was a differentially pumped molecular beam machine, with the detection chamber enclosed inside the source chamber.[35] A time-of-flight mass spectrometer in the detection chamber also served as the pulsed field ionization zero kinetic energy photoelectron spectrometer. Triphenylene (Aldrich) was housed and heated to 260 °C in the pulsed valve located in the source chamber. The vapor of the sample was seeded in 400 Torr of argon and co-expanded into vacuum through a pulsed valve with a 1 mm orifice. After passing through a 2 mm skimmer, the cooled sample reached the detection chamber for laser excitation and ionization. The laser systems for the REMPI experiment included two Nd:YAG (Spectra Physics, GCR 190 and GCR 230) pumped dye lasers (Laser Analytical System, LDL 20505 and LDL 2051), both equipped with frequency doublers. The excitation laser in the 304–340 nm range had a typical pulse energy of more than 1.0 mJ/pulse with a bandwidth of 0.5 cm^{-1}. The ionization laser in the 287–301 nm range had a pulse energy of ∼1 mJ/pulse with a bandwidth of 0.3 cm^{-1}. The absolute wavelength of each laser was calibrated using an iron hollow-cathode lamp filled with neon. The pump laser and ionization laser were set to counter-propagate, and the light path, the flight tube, and the molecular beam were mutually perpendicular. Two delay generators (Stanford Research, DG 535) controlled the timing of the lasers and the pulsed valve, and the optimal signal was obtained under temporal overlap between the pump and ionization lasers. In the ZEKE experiment, molecules were excited to high Rydberg states for 400 ns in the presence of a small constant DC spoiling field, after which ionization and extraction were achieved by a pulsed electric field of ∼2 V/cm.

The Gaussian 09 suite[45] was used to optimize the molecular structure, to obtain vibrational frequencies, and to simulate the observed vibrational distribution from REMPI. For the ground state of the neutral and the cationic state, density functional theory (DFT) calculations using the B3LYP functional were performed with the 6-31+G basis set. The excited states S_1 and S_2 were calculated using both time dependent density functional theory (TDDFT) with the B3LYP functional and the 6-31+G basis set as well as configuration interaction singles (CIS) with the 6-31+G basis set. Details of the calculations will be provided in Results section.

RESULTS

Two-color 1+1′ REMPI spectroscopy

Figure 1 shows the two-color REMPI spectrum of triphenylene near the origin of the $S_1 \leftarrow S_0$ electronic transition. The ionization laser was set at 35 090 cm^{-1} and the excitation laser was scanned for resonant transitions. Table I includes the observed vibronic transitions, the corresponding calculated values from Gaussian 09 using TDDFT at the 6-31+G level, and the symmetry assignments in the D_{3h} point group. The labeling is by symmetry species and by numbering each species independently from low to high frequencies, a convention used by several groups since 2008.[33,46] As will be discussed later, the electronic transition is dipole forbidden, resulting in no origin band, thus assignment of the origin is based on assignment of the vibronic bands. Our current value of 29 618 cm^{-1} for the origin of the electronic transition is in excellent agreement with the work of Kokkin *et al.* in the gas phase,[47] but it is shifted by ∼470 cm^{-1} from the report of Merle, Campion and El-Sayed.[39] The blue shift of the latter work has been attributed to the effect of the *n*-heptane matrix. In Figure 1, the spectrum is shifted to the electronic origin to emphasize the vibronic structure. Typically, calculated vibrational frequencies for electronically excited states are over estimates, which can be corrected with a small scaling factor. In this case, a scaling factor of 0.964 has been used based on a least squares fit between the experimental and the putative theoretical values, and the resulting correlation of determination of the linear regression is 0.9999. The value of the scaling factor is within the typical range for calculations using the B3LYP functional.[31–37]

A feature of Gaussian 09 is inclusion of Herzberg-Teller coupling for simulations of vibronic transitions, often with very reasonable accuracy for intensity distributions.[45] The resulting spectrum can further assist with the assignment of the observed REMPI transitions. However, a problem with Gaussian 09, regardless of methods of calculation, is the uncertainty in the energy of closely spaced excited electronic states.[31–37] Consequently in Figure 2, we show the simulated spectra with Herzberg-Teller coupling for both the $S_1 \leftarrow S_0$ and the $S_2 \leftarrow S_0$ transitions of triphenylene. Although the lack of an origin band could potentially complicate the assignment of the spectrum, fortunately in this case, the agreement between simulation and experiment in Figure 2 is quite reasonable. The observed vibronic bands do indeed correspond to those from the $S_1 \leftarrow S_0$ transition.[38–40,47]

The assignment in Table I is based on several considerations. First, even with HT coupling, selection rules for electric dipole transitions are still obeyed, hence only vibronic transitions with an overall symmetry species of e′ are allowed. Second, given the symmetry constraint, the assignment of many low frequency bands is indisputable because of the discrete quantized fundamental frequencies. Third, the spectroscopic simulation presented in Figure 2 offers theoretical guidance for the observed transitions. Nevertheless, there are a few transitions that have unusually large deviations, but in general, the agreements between theory and experiment and between our assignment and two other previous works using different methods are quite satisfactory.[39,47] The assignment for the transition at 1417 cm^{-1} is based on a comparison with the calculated spectrum, hence it is different from that of a previous report.[47]

ZEKE spectroscopy

By setting the first laser at one of the intermediate states identified in the REMPI experiment and scanning the second laser, we have obtained the pulsed field ionization ZEKE spectra of triphenylene. Figures 3 and 4 show the ZEKE spectra via the first six vibronic transitions labeled in bold-faced font in Figure 1. Efforts of using intermediate states with vibrational energies higher than 900 cm^{-1} have yielded no

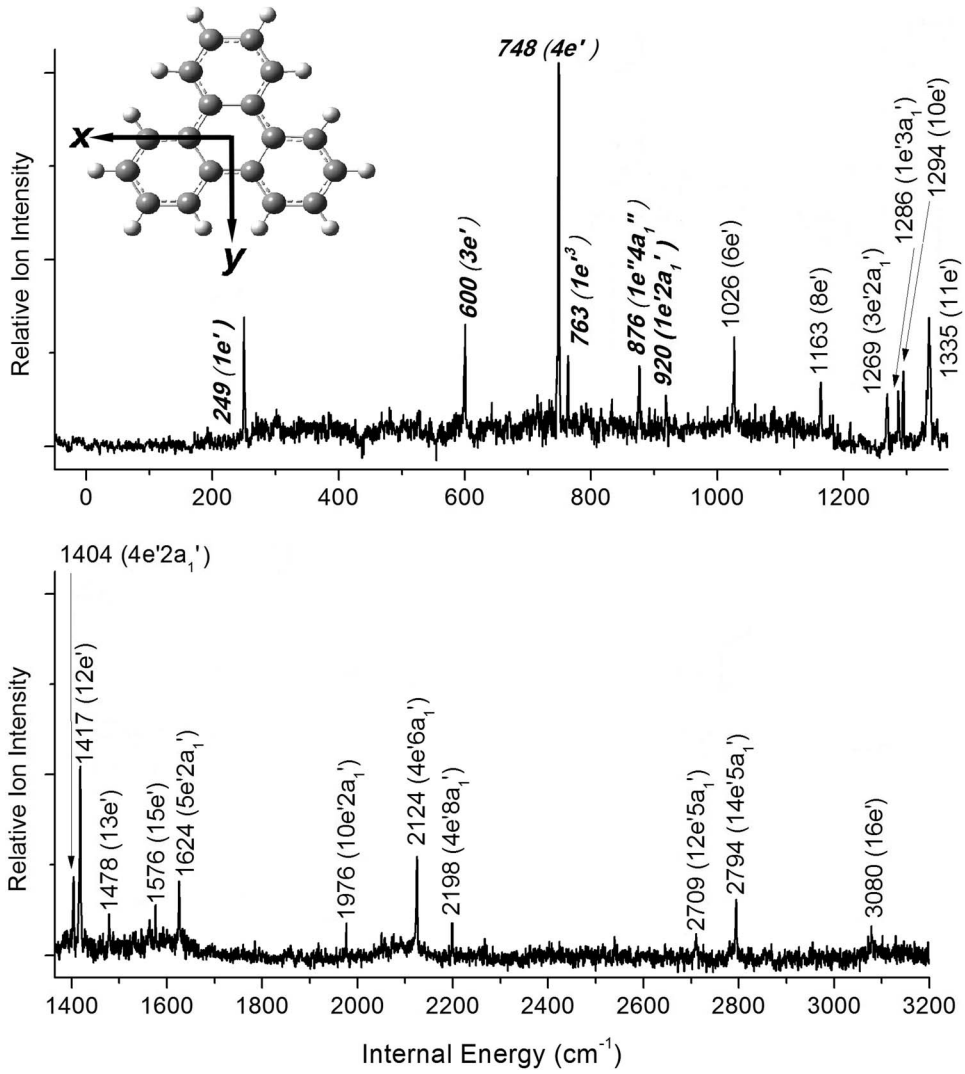

FIG. 1. REMPI spectrum of triphenylene shifted by 29 618 cm^{-1}, the energy for the origin of the S_1 state. The energy region below 180 cm^{-1} was scanned with 180 laser shots for each data point in a failed attempt to observe the origin band, while the rest of the spectrum was the average of 100 laser shots. Modes in bold-faced italic fonts are the intermediate vibronic transitions which have yielded ZEKE spectra. The molecular structure with designations of axes is also included.

ZEKE signal. This kind of internal energy "cutoff" seems typical for the ZEKE experiments that we have performed.[31–37] The inconsistent signal-to-noise ratio (S/N) of Fig. 4(c) is due to the extra effort in the scan of the central region (marked by two arrows): while the rest of the region and the rest of all the ZEKE spectra have been results of averages over 100 laser shots, this central region has been the average of 170 laser shots per data point. The data have also been recorded in different days, and slight variations in experimental parameters could also contribute to the difference in the S/N of the spectrum. The adiabatic origin of the cationic ground state is tentatively assigned to be 63 365 ± 7 cm^{-1}, corresponding to the observed lowest frequency band and taking into consideration the shift caused by the delayed electric pulse for ionization. This value is about 200 cm^{-1} below that reported by Boschi, Clar and Schmidt via photoelectron spectroscopy.[48] The discrepancy is not surprising since the higher spectral resolution of ZEKE than that of typical photoelectron spectroscopy can effectively remove interferences from hot bands and from external electric and magnetic fields.

Compared with the ZEKE spectrum of benzene[49,50] where coupling among different JT active modes is extensive, the ZEKE spectra of triphenylene are sparse and contain a recognizable pattern – a dominant single cluster of transitions. Jahn-Teller coupling results in splittings of vibrational levels, thus the individual transitions within each cluster could be related to the same doubly degenerate vibrational band of the intermediate state. This single cluster of transitions of each spectrum is thus an indicator of a propensity in preserving the vibrational excitation of the intermediate state.[31–37,51,52]

Full assignment of the observed ZEKE transitions in the presence of Jahn-Teller distortion requires calculations similar to those of Applegate and Miller on the analysis of the ZEKE spectrum of benzene.[50] The inset of the bottom panel in Fig. 3 shows three transitions, two of which constitute a closely spaced doublet (7 cm^{-1} apart), and the 3rd transition is nearly 50 cm^{-1} above the doublet. This pattern is very similar to that of the ZEKE spectrum obtained via the $2^1 18^1$ vibrational level of the S_1 state of benzene.[50] A similar pattern is also observable in the inset of the middle panel of Fig. 3,

TABLE I. Observed vibrational bands for the S_1 (A_1') state of triphenylene. Bands in bold-faced italic font are intermediate states which have yielded ZEKE spectra (units: cm^{-1}, uncertainty: $\pm 5\ cm^{-1}$).

Experimental	Calculation[a]	Assignment	Matrix isolation[b]	LIF[c]
249	***252***	***1e′***	249	247 (1e′)
600	***609***	***3e′***	616	597 (3e′)
748	***748***	***4e′***	769	745 (4e′)
763	***755***	***1e′³***	789	
876	***866***	***1e″4a₁″***		
920	***925***	***1e′2a₁′***		
1026	1030	6e′	1036	
1163	1161	8e′	1172	
1269	1282	3e′2a$_1$′	1271	
1286	1306	1e′3a$_1$′		
1294	1307	10e′		
1335	1326	11e′	1336	1332 (11e′)
1404	1405	4e′2a$_1$′	1410	1402 (4e′2a$_1$′)
1417	1424	12e′	1437	1414 (12e′)
1478	1483	13e′	1480	
1576	1573	15e′	1576	
1624	1626	5e′2a$_1$′		
1976	1980	10e′2a$_1$′	1997	1973 (3e′7a$_1$′)
2124	2101	4e′6a$_1$′	2117	
2198	2197	4e′8a$_1$′	2184	
2709	2698	12e′5a$_1$′	2697	
2794	2790	14e′5a$_1$′	2777	2784 (12e′7a$_1$′)
3080	3085	16e′		

[a]Including a scaling factor of 0.964.
[b]Matrix isolation spectroscopy in *n*-heptane crystal with a scaling factor of 0.98.[39]
[c]Gas-phase laser induced fluorescence.[47]

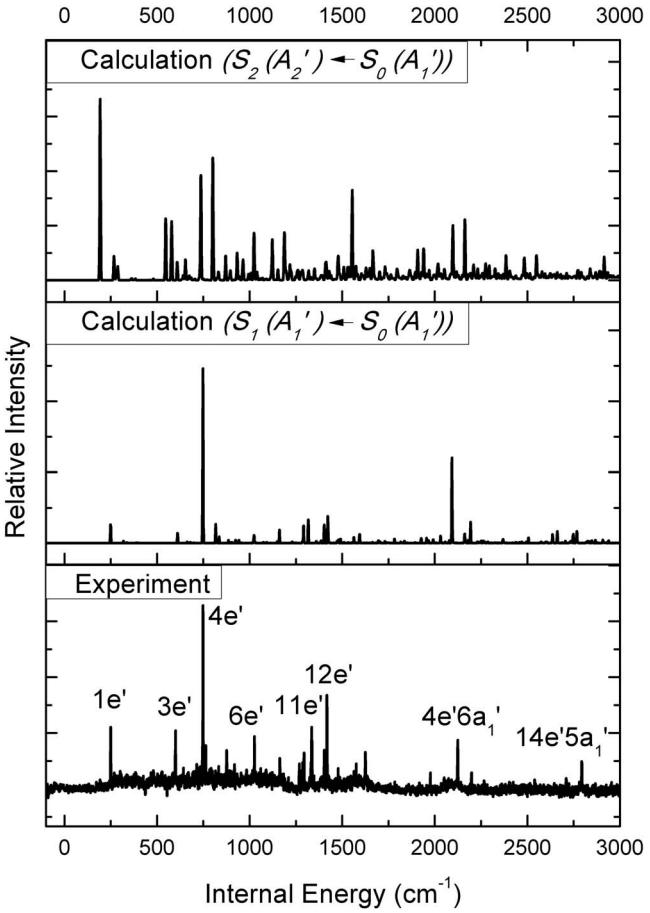

FIG. 2. Comparison between the experimental REMPI spectrum and the simulation using Gaussian 09 including Herzberg-Teller coupling.

although the doublet feature is now a triplet. However, the analysis of Applegate and Miller did not explicitly associate the observed vibrational transition with the unperturbed degenerate state.[50] In so doing, some physical insights related the ionization process could be missed.

In this work, we adopt the approach of Keszthelyi *et al.*[43,53] by simply using the unperturbed vibrational frequencies from our DFT calculation for a preliminary analysis. The advantage of this treatment is the explicit symmetry information of the assigned vibrational transitions in the deformed molecular frame. Based on our calculations using unrestricted Hartree-Fock, Møller–Plesset second order perturbation theory, coupled cluster configuration interactions with single and double substitutions, and density functional methods, the vibrational frequencies from the unperturbed electronic states in the C_{2v} symmetry that constitute the Jahn-Teller pair are almost identical (within 1 cm^{-1}). By using the frequencies of a single cationic state from our DFT calculation as a guide, we offer a tentative assignment as that listed in Table II. As seen in the insets of Fig. 3, the current assignment leaves out many details revealed in the spectra. Nevertheless, the agreement in frequency between calculation and experiment in Table II is surprisingly good. A similar situation has also been reported by Keszthelyi *et al.*[43] on Raman spectroscopy of triphenylene cations. For bands with moderately high vibrational energies, we could attribute the agreement to the freedom in using combinations of low frequency modes just to match the transition wavenumbers, but this reason cannot be used to negate the agreement of the lower energy bands. One possibility of this surprisingly good agreement might be related to the strength of coupling specific to these vibrational modes. According to the report by Kato and Yamabe,[42] only three e′ modes are primarily responsible for JT coupling, and none of the three are accessed in the REMPI spectrum of Figure 1.

With this crude treatment, we can follow the transformation of vibrational modes from the S_1 to the D_0 states thereby peeking into the mechanism of ionization. We start by considering that when the electronic state exhibits JT distortion from D_{3h} to C_{2v}, the e′ vibrational modes resolve into a_1 and b_2 modes. We can then construct a resolution map from the e′ modes of the intermediate state to the a_1 and b_2 modes of the final ionic state. This correlation will in turn guide or confirm the vibrational assignment of both the REMPI and ZEKE spectra. Using GaussView[45] for visualization of the displacement vectors and using vibrational frequencies for guidance, we have concluded on a list of correlated vibrational modes as shown in Table III. It is important to note that the a_1 modes of C_{2v} arise from both the a_1' as well as the e′ modes of D_{3h}, and the b_2 modes of C_{2v} arise from both the e′ and the a_2' modes of D_{3h}. This means that in the resolution table of the e′ modes, the numbering of the modes in C_{2v} is not necessarily consecutive.

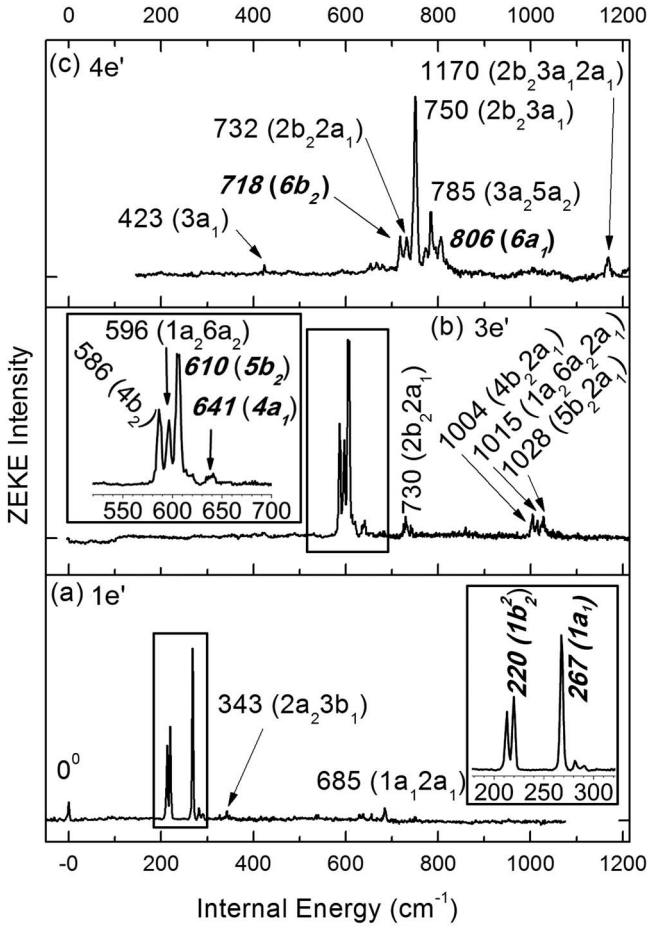

FIG. 3. Experimental ZEKE spectra from intermediate vibronic states: (a) 1e′, (b) 3e′, and (c) 4e′, shifted by 63 365 cm^{-1}. Modes in bold-faced italic font are the correlated diagonal modes.

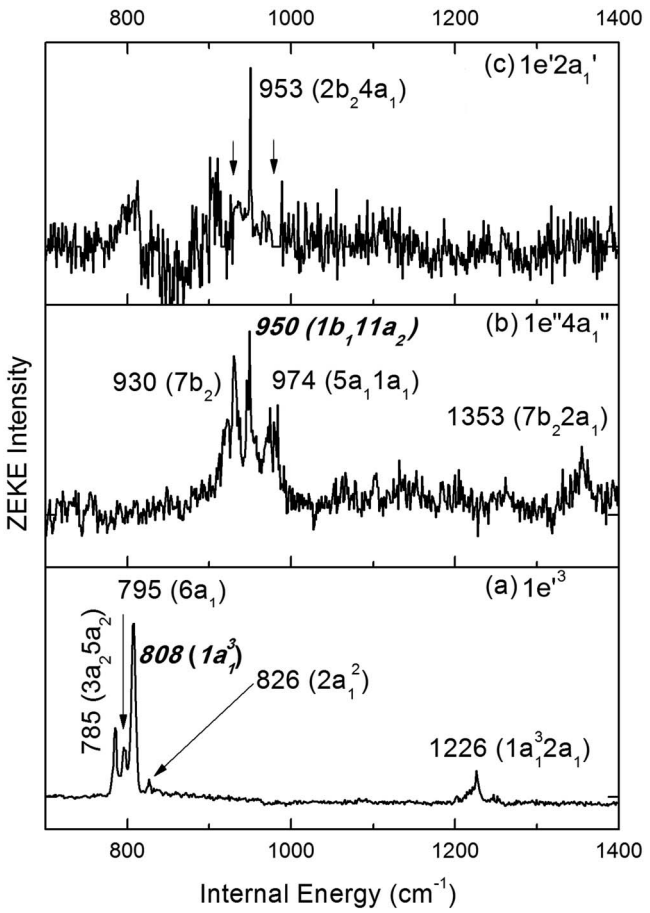

FIG. 4. Experimental ZEKE spectra from intermediate vibronic states: (a) 1e′3, (b) 1e″4a1″, and (c) 1e′2a1′, shifted by 63 365 cm^{-1}. The top two panels are scaled up by a factor of 5. The inconsistent signal-to-noise ratio in panel (c) is due to the extra effort (170 laser shots vs. 100 laser shots per data point and perhaps better alignment on the day of the attempt) during the scan of the central region. Modes in bold-faced italic font are the correlated diagonal modes.

Figure 5 shows the displacement vectors of the lowest frequency e′ mode and the correlated a_1 and b_2 modes. This e′ mode in D_{3h} can be regarded as two degenerate in-plane vibrations, one of which is symmetric about the vertical plane σ_v (a_1) and the other is anti-symmetric (b_2). The b_2 mode in C_{2v} involves wagging of one terminal (top) ring relative to the somewhat rigid phenanthrene substructure, while the a_1 mode looks like scissoring of the two rings within the phenanthrene substructure while the top ring staying relatively still. In the ZEKE spectrum of Figure 3(a), the strongest transition from the e′ mode of the intermediate state is assigned as the a_1 mode of the cation. Although further calculations using the Applegate and Miller approach[50] will inevitably shift the theoretical transition frequency by introducing JT coupling terms, our current approach should capture the predominant feature of the observed transition.

Many previous studies of ZEKE spectroscopy via resonantly excited states have reported a propensity rule, i.e., the strongest transition in the ZEKE spectrum can be assigned as the same vibrational mode as that of the intermediate state.[31–37,51,52] If the propensity rule holds for triphenylene, we would expect many of the correlated a_1 and b_2 modes to be present in the ZEKE spectra. This is indeed the result from Figures 3 and 4, where the intense clusters of transitions contain one or both of the correlated modes of the intermediate state (labeled in bold). However, in Figures 3 and 4, weaker replicas of the strong cluster of transitions are also observable, and these replicas can be assigned as combinations of the original cluster of transitions with a $2a_1$ transition at 416 cm^{-1}. Clearly the Franck-Condon factor from the S_1 intermediate state to the cationic state D_0 is not totally diagonal.

DISCUSSIONS

The S_1 electronic state and vibrational assignment

The symmetry of several low lying electronic states and the corresponding electronic orbitals are informative in understanding the origin of the vibronic coupling in triphenylene. Both the highest occupied molecular orbital (HOMO) and the lowest unoccupied molecular orbital (LUMO) are e″ in symmetry, and every e″ orbital consists of a symmetric and anti-symmetric molecular orbital with respect to the vertical mirror plane σ_v (symmetry plane shown in Figure 5). Excitation from the doubly degenerate HOMO to the doubly degenerate LUMO can result in four possible transitions, corresponding to three possible electronic states with symmetry terms of A_1', A_2', and E′. Based on the output from TDDFT calculations,

TABLE II. Observed vibrational bands of the D_0 state of triphenylene from several intermediate vibronic transitions. The bands in bold-faced italic font are the correlated diagonal bands of the intermediate state (units: cm^{-1}, uncertainty: $\pm 7\ cm^{-1}$).

1e′	3e′	4e′	$1e'^3$	$1e''4a_1''$	$1e'2a_1'$	Calc	Assignment
220						238	$1b_2^2$
267						265	$1a_1$
343						352	$2a_2 3b_1$
		423[a]				430	$3a_1$
	586					584	$4b_2$
	596[a]					594	$1a_2 6a_2$
	610					623	$5b_2$
	641					641	$4a_1$
685[a]						681	$1a_1 2a_1$
		718				698	$6b_2$
	730	732				735	$2b_2 2a_1$
		750				749	$2b_2 3a_1$
		785	785			778	$3a_2 5a_2$
		806	795			801	$6a_1$
			808			795	$1a_1^3$
			826			832	$2a_1^2$
				930		940	$7b_2$
				950		963	$1b_1 11a_2$
					953	960	$2b_2 4a_1$
				974		975	$5a_1 1a_1$
	1004					1000	$4b_2 2a_1$
	1015					1010	$1a_2 6a_2 2a_1$
	1028					1039	$5b_2 2a_1$
		1170				1165	$2b_2 3a_1 2a_1$
			1226			1211	$1a_1^3 2a_1$
				1353		1356	$7b_2 2a_1$

[a]Modes that are observed in the matrix isolation resonant Raman experiment.[43]

the transition to the S_1 state contains equal contributions from transitions between orbitals of the same symmetry, hence the S_1 state can be assigned as A_1'. The situation for the transition to the S_2 state is the opposite, consisting of equal contributions between molecular orbitals of different symmetry, hence the S_2 state can be assigned as A_2'. The transitions to

TABLE III. The e′ (D_{3h}) modes and the correlated a_1 and b_2 (C_{2v}) modes with the calculated frequencies in parenthesis (units: cm^{-1}).

S_1 (D_{3h}) modes[a]	Correlated D_0 (C_{2v}) modes
1e′ (252)	$1b_2$ (119) $1a_1$ (265)
2e′ (395)	$2b_2$ (319) $2a_1$ (416)
3e′ (609)	$5b_2$ (623) $4a_1$ (641)
4e′ (748)	$6b_2$ (698) $6a_1$ (801)
5e′ (951)	$7b_2$ (940) $7a_1$ (1012)
6e′ (1030)	$9b_2$ (1088) $8a_1$ (1068)
7e′ (1081)	$10b_2$ (1111) $10a_1$ (1141)

[a]Including a scaling factor of 0.964.

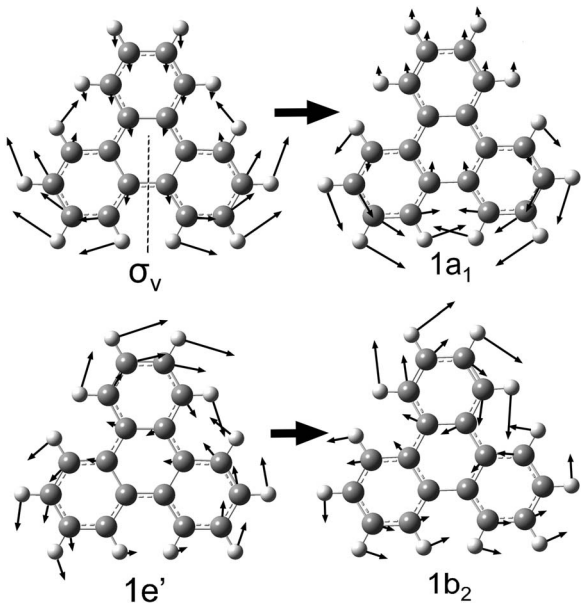

FIG. 5. The 1e′ vibrational mode of S_1 (D_{3h}) and its resolution into the b_2 and a_1 modes of D_0 (C_{2v}). The displacement vectors (thinner arrows) are included as well as the vertical mirror plane σ_v (dashed line).

the S_3 state consist of a degenerate pair, which confirms the E′ assignment for S_3.[38] The transition dipole for the D_{3h} group is either e′ or a_2'', hence both S_1 and S_2 are electric dipole forbidden. Any observed vibronic transitions to S_1 are therefore due to vibronic coupling with the dipole allowed S_3 state.

It might seem surprising that all observed vibronic bands from REMPI are results of coupling to the third electronically excited state S_3. The energy difference between S_3 and S_1 is $\sim$7000 cm^{-1} by our calculation, which agrees with that of Chojnacki *et al.*[38] This energy gap is the largest although not totally out of reason when compared with those in other PAHs that we have studied. For example, the energy gap is 1200 cm^{-1} for B*a*P,[34] 3000 cm^{-1} for pyrene,[35] and 5000 cm^{-1} for B*e*P.[31] However, all of these PAHs couple to the S_2 electronic state. We have previously concluded and once again confirm in this study that the degree of Herzberg-Teller coupling does not necessarily correlate with the energy gap.[31–37,51,52] A somewhat surprising realization is that despite the large energy difference and the complete electric dipole forbidden nature of the S_1 state, the vibronic transitions are strong and the corresponding Rydberg states are stable enough for further ZEKE spectroscopy.

With the exception of a missing origin band, the REMPI spectrum of triphenylene is similar to those of other PAHs that our group has studied.[31–37,51,52,54,55] The observed vibrational modes are in-plane, and the simulated spectrum captures the essence of the experimental data, despite the dominance of vibronic coupling. Based on our calculation, the molecular frame hardly changes upon excitation, expanding only by about half a percent in all directions because of the increased nodal character in the excited electronic state.[31–37]

The first electronically excited state of triphenylene has been studied by several groups using a variety of techniques including gas phase laser induced fluorescence (LIF)[47] and matrix isolation spectroscopy.[38–41] The LIF study by Kokkin

et al. is in close agreement with our work in terms of frequency, intensity, and assignment, as shown in Table I.[47] The frequencies from matrix isolation spectroscopy at 1.6 K[39] are also included in Table I for comparison. In general, frequencies from MIS experiments either at 77 K[38,41] or at 1.6 K[39] require a scaling factor of 0.98 to agree with the corresponding values from gas phase studies. The scaling factor is indicative of deformation of the molecular frame relative to that of free space gas phase molecules.[39,40] This effect is not too surprising given the seemingly floppy shape of the molecular frame. Furthermore, all MIS studies have shown a small but observable origin band, implying that the symmetry of the electronic state has perhaps been distorted.[38–40] Based on polarization analysis, Lamotte *et al.* have indeed confirmed the symmetry of the S_1 state to be C_{2v} in their matrix.[40]

Geometry and vibrational assignment of the D_0 state

After photoionization, the resulting electron configuration for triphenylene is $(e'')^3$, a prime candidate for Jahn-Teller distortion. There have been several studies, both theoretical and experimental, indicating that both the cation and anion are of C_{2v} symmetry.[42–44,56,57] In particular, Keszthelyi *et al.*[43] have reported the resonant Raman spectroscopy of triphenylene cation along with Hartree-Fock and density functional calculations, and the authors have simulated the experimental spectrum based on parameters from the C_{2v} molecular frame.[43]

Jahn-Teller distortion results in two electronic states A_2 and B_1 for triphenylene. Based on calculations of our own and those of Keszthelyi *et al.*[43] using a range of methods, the two states are nearly degenerate. In the A_2 state, one of the arms is compressed, while in the B_1 state, the arm is elongated. We have then calculated the energy of the D_{3h} conical intersection by averaging the geometric parameters of the Jahn-Teller pair, and the resulting barrier is $\sim$1000 cm^{-1}. This value is on par with that from Keszthelyi *et al.*[43] Given the scope of the current work and our emphasis for the correlation between the vibrational levels of the intermediate state and those of the final state, we will leave the full Jahn-Teller analysis for the future.

Interestingly, the change in symmetry only exerts minor effect on the actual dimension of the molecular frame, resulting in observable propensity in preserving the vibrational excitation of the intermediate state. This result is not too surprising given the relatively large number of rings of triphenylene thereby its capacity to accommodate the positive charge of the cation.

There are some similarities between our data and those from the resonant Raman experiment of Keszthelyi *et al.*[43] While the intensities should be different between these two experiments because of different selection rules, some common vibrational modes particularly the a_1 modes should be observable in both experiments. In Table II, three reported a_1 modes from Keszthelyi *et al.*[43] are marked with asterisks. However in our case, the two higher frequency bands are better assigned as combination bands based on correlations with the intermediate vibrational level. It is possible that the bands observed in the matrix are different from ours since no matrix effect has been considered in the original report.

Comparisons with other PAHs

With the exception of JT distortion, triphenylene is in many ways similar to the other PAHs that we have studied.[31–37] The observable modes from both the S_1 and D_0 electronic states are restricted to in-plane vibrations, and the scaling factor for the vibrational frequency of the S_1 state is also within the range of expected values.[31–37] In pyrene and a few cata-condensed PAHs,[32,35,36] we have observed out-of-plane vibrations due to vibronic coupling, and in all cases, the out-of-plane modes have been electric dipole allowed because of the symmetry of the coupled higher electronic state. Although the degree of vibronic coupling is extraordinary in triphenylene, no out-of-plane modes are allowed because of the symmetry of the S_3 (E') electronic state. Hence the existence and intensity of out-of-plane modes are not indicative of molecular rigidity.

Coronene and benzene are both similar to triphenylene in that they are highly symmetric PAHs and they exhibit JT distortion upon ionization. In terms of structural distortion, based on our calculation, the $D_0 \leftarrow S_0$ transition in triphenylene shrinks the overall dimension along one of the principal axes by less than 0.25% and expands the dimension in the perpendicular direction by a little less than 0.5%. The structural change in coronene is similar, consistent with the trend that larger molecules tolerate more disturbances in the electronic structure. In contrast, the JT distortion of benzene cation is much more pronounced, with the dimension along the elongated axis increasing by 4%. Consequently, the ZEKE spectrum of benzene contains an extensive distribution of vibrational bands, including several out-of-plane modes,[49,50] while the ZEKE spectra of triphenylene mostly contain diagonal vibrational bands.

CONCLUSIONS

The vibrational information of triphenylene for both the first electronically excited state and the cationic ground state is reported based on REMPI and ZEKE spectroscopy. The $S_1 \leftarrow S_0$ electronic transition is electric dipole forbidden and all vibrational bands are results of vibronic coupling with a high lying S_3 (E') electronic state. Using Gaussian 09, we are able to simulate the vibronic spectrum of the S_1 state, from which we have determined the origin of the S_1 state to be $29\,618 \pm 5$ cm^{-1}. Removal of an electron results in a symmetry change from D_{3h} to C_{2v}, but the actual changes in structural parameters are still small. Based on a resolution of the intermediate e' modes from D_{3h} to the a_1 and b_2 modes of C_{2v}, some transitions in the ZEKE spectra can be tentatively assigned, and the propensity of preserving the vibrational excitation of the intermediate state can be observed. No ZEKE signal has been observed from intermediate states with vibrational energy excesses higher than 900 cm^{-1}, similar to many of the PAHs we have investigated. Given the complexity of the ZEKE spectra, however, a complete understanding

and assignment will require a detailed calculation of vibronic wavefunctions of the Jahn-Teller pair, a task that awaits future effort.

ACKNOWLEDGMENTS

This work is supported by the National Aeronautics and Space Administration under Award No. NNX09AC03G.

[1]L. E. Smith, M. F. Denissenko, W. P. Bennett, H. Li, S. Amin, M.-S. Tang, and G. P. Pfeifer, J. Natl. Cancer Inst. **92**, 803 (2000).
[2]E. Kriek, M. Rojas, K. Alexandrov, and H. Bartsch, Mutat, Res., Fundam. Mol. Mech. Mutagen. **400**, 215 (1998).
[3]R. G. Harvey, *Polycyclic Aromatic Hydrocarbons: Chemistry and Carcinogenicity* (Cambridge University Press, London, 1991).
[4]P. Bréchignac, T. Pino, and N. Boudin, Spectrochim. Acta, Part A **57**, 745 (2001).
[5]F. Salama, G. A. Galazutdinov, J. Krelowski, L. J. Allamandola, and F. A. Musaev, Astrophys. J. **526**, 265 (1999).
[6]A. Li, in *PAHs in Comets: An Overview. Deep Impact as a World Observatory Event – Synergies in Space, Time, and Wavelength*, edited by H. U. Käufl and C. Sterken (Springler, Berlin, 2009), p. 161.
[7]Y. M. Rhee, T. J. Lee, M. S. Gudipati, L. J. Allamandola, and M. Head-Gordon, Proc. Natl. Acad. Sci. U.S.A. **104**, 5274 (2007).
[8]E. Peeters, L. J. Allamandola, D. M. Hudgins, S. Hony, and A. G. G. M. Tielens, Astron. Soc. Pac. Conf. Ser. **309**, 141 (2004).
[9]G. Malloci, G. Mulas, and P. Benvenuti, Astron. Astrophys. **410**, 623 (2003).
[10]G. Mulas, G. Malloci, and P. Benvenuti, Astron. Astrophys. **410**, 639 (2003).
[11]A. Li and J. I. Lunine, Astrophys. J. **594**, 987 (2003).
[12]L. J. Allamandola, A. G. G. M. Tielens, and J. R. Barker, Astrophys. J. **290**, L25 (1985).
[13]A. Leger and J. L. Puget, Astron. Astrophys. **137**, L5 (1984).
[14]M. P. Bernstein, J. P. Dworkin, S. A. Sandford, G. W. Cooper, and L. J. Allamandola, Nature (London) **416**, 401 (2002).
[15]E. L. Shock and M. D. Schulte, Nature (London) **343**, 728 (1990).
[16]S. G. Wakeham, C. Schaffner, and W. Giger, Geochim. Cosmochim. Acta **44**, 415 (1980).
[17]D. M. Hudgins and S. A. Sandford, J. Phys. Chem. A **102**, 344 (1998).
[18]D. M. Hudgins and S. A. Sandford, J. Phys. Chem. A **102**, 329 (1998).
[19]S. R. Langhoff, C. W. Bauschlicher, Jr., D. M. Hudgins, S. A. Sandford, and L. J. Allamandola, J. Phys. Chem. A **102**, 1632 (1998).
[20]D. M. Hudgins and L. J. Allamandola, J. Phys. Chem. A **101**, 3472 (1997).
[21]D. M. Hudgins and L. J. Allamandola, J. Phys. Chem. **99**, 3033 (1995).
[22]D. M. Hudgins and L. J. Allamandola, J. Phys. Chem. **99**, 8978 (1995).
[23]H. S. Kim, D. R. Wagner, and R. J. Saykally, Phys. Rev. Lett. **86**, 5691 (2001).
[24]J. Oomens, A. J. A. Van Roij, G. Meijer, and G. Von Helden, Astrophys. J. **542**, 404 (2000).
[25]M. C. R. Cockett and K. Kimura, J. Chem. Phys. **100**, 3429 (1994).
[26]M. Vala, J. Szczepanski, F. Pauzat, O. Parisel, D. Talbi, and Y. Ellinger, J. Phys. Chem. **98**, 9187 (1994).
[27]J. Szczepanski and M. Vala, Astrophys. J. **414**, 646 (1993).
[28]K. Zhang, B. Guo, P. Colarusso, and P. F. Bernath, Science (Washington, D. C.) **274**, 582 (1996).
[29]M. F. Denissenko, A. Pao, M. Tang, and G. P. Pfeifer, Science (Washington, D. C.) **274**, 430 (1996).
[30]E. W. Schlag, *ZEKE Spectroscopy* (Cambridge University Press, London, 1998).
[31]C. Harthcock, J. Zhang, and W. Kong, Chem. Phys. Lett. **556**, 23 (2013).
[32]J. Zhang, C. Harthcock, and W. Kong, J. Phys. Chem. A **116**, 7016 (2012).
[33]J. Zhang, C. Harthcock, and W. Kong, J. Phys. Chem. A **116**, 1551 (2012).
[34]J. Zhang, C. Harthcock, F. Han, and W. Kong, J. Chem. Phys. **135**, 244306 (2011).
[35]J. Zhang, F. Han, and W. Kong, J. Phys. Chem. A **114**, 11117 (2010).
[36]J. Zhang, F. Han, L. Pei, W. Kong, and A. Li, Astrophys. J. **715**, 485 (2010).
[37]J. Zhang, L. Pei, and W. Kong, J. Chem. Phys. **128**, 104301 (2008).
[38]H. Chojnacki, Z. Laskowski, A. Lewanowicz, Z. Ruziewicz, and R. Wandas, Chem. Phys. Lett. **124**, 478 (1986).
[39]A. M. Merle, A. Campion, and M. A. El-Sayed, Chem. Phys. Lett. **57**, 496 (1978).
[40]M. Lamotte, S. Risemberg, A. M. Merle, and J. Joussot-Dubien, J. Chem. Phys. **69**, 3639 (1978).
[41]Z. Ruziewicz, Acta Phys. Polon. **28**, 389 (1965).
[42]T. Kato and T. Yamabe, Chem. Phys. Lett. **403**, 113 (2005).
[43]T. Keszthelyi, G. Balakrishnan, R. Wilbrandt, W. A. Yee, and F. Negri, J. Phys. Chem. A **104**, 9121 (2000).
[44]M. G. Townsend and S. I. Weissman, J. Chem. Phys. **32**, 309 (1960).
[45]M. J. Frisch, G. W. Trucks, H. B. Schlegel *et al.*, GAUSSIAN 09, Revision A.1, Gaussian Inc., Wallingford, CT, 2009.
[46]O. Birer, P. Moreschini, and K. K. Lehmann, Phys. Chem. Chem. Phys. **10**, 1648 (2008).
[47]D. L. Kokkin, N. J. Reilly, T. P. Troy, K. Nauta, and T. W. Schmidt, J. Chem. Phys. **126**, 084304 (2007).
[48]R. Boschi, E. Clar, and W. Schmidt, J. Chem. Phys. **60**, 4406 (1974).
[49]R. Lindner, K. Mueller-Dethlefs, E. Wedum, K. Haber, and E. R. Grant, Science (Washington, D. C.) **271**, 1698 (1996).
[50]B. E. Applegate and T. A. Miller, J. Chem. Phys. **117**, 10654 (2002).
[51]Y. He, C. Wu, and W. Kong, J. Chem. Phys. **120**, 7497 (2004).
[52]Y. He, C. Wu, and W. Kong, J. Chem. Phys. **121**, 3533 (2004).
[53]W. H. Henneker, A. P. Penner, W. Siebrand, and M. Z. Zgierski, J. Chem. Phys. **69**, 1884 (1978).
[54]Y. He and W. Kong, J. Chem. Phys. **124**, 204306 (2006).
[55]Y. He and W. Kong, J. Chem. Phys. **122**, 244302 (2005).
[56]S. R. Langhoff, J. Phys. Chem. **100**, 2819 (1996).
[57]Z. H. Khan, Can. J. Spectrosc. **23**, 8 (1978).